Final Technical Report

External Grant Award Number:
G14AP00020
Recipient:
Optim Seismic Data Solutions, Inc.

Principal Investigators:
Aasha Pancha
Optim SDS, 200 South Virginia Street, Suite 560, Reno, NV, 89501
Telephone (775) 236-5869 Fax:(775) 324-5662
Now: at Victoria University of Wellington, Aasha.Pancha@vuw.ac.nz
Satish Pullammanappallil
Optim SDS, 200 South Virginia Street, Suite 560, Reno, NV, 89501
Telephone.: (775) 236-5891 Fax:(775) 324-5662 satish@optimsoftware.com

Title:
Determination of 3D-velocity structure across the northeastern portion of the Reno area basin

NEHRP Elements(s)
Element I: National and regional earthquake hazards assessments
Keywords: Site effects, Basin effects, Ground motions, Seismic Zonation, Engineering seismology

Start date: January 2014
End Date: December 2014

Determination of 3D-velocitystructure across the northeastern portion of the Reno-Area Basin

Aasha Pancha
Optim SDS, 200 South Virginia Street, Suite 560, Reno, NV, 89501
Telephone (775) 236-5869 Fax:(775) 324-5662
Now: at Victoria University of Wellington, Aasha.Pancha@vuw.ac.nz
Satish Pullammanappallil
Optim SDS, 200 South Virginia Street, Suite 560, Reno, NV, 89501
Telephone.: (775) 236-5891 Fax:(775) 324-5662 satish@optimsoftware.com

ABSTRACT

Estimation of shallow shear velocities is a key element in the assessment of sites for potential earthquake ground shaking and damage. We assess shear-wave velocities across the northwestern portion of the Reno-area basin where gravity indicates a major sub-basin. Little structural and velocity data is available for this region. Existing velocity models are limited in resolution to intervals of 1 km to 3 km. As a result, 3D basin details are currently insufficient for scenario modeling, an essential component of seismic hazard evaluation. Trial scenario models run at the University of Nevada, Reno (UNR) for the 2008 Mogul M5 event are failing to predict recorded ground motions, even to a factor of two. Through this grant shear velocity to depths of up to 1000 m were measured using refraction-microtremor (ReMi) arrays with 50 m depth resolution. This was achieved through the deployment of standalone wireless instruments to record ambient urban noise along two orthogonal arrays. Based on data quality and resolution observed during the pilot study undertaken through G12AP20026 (Pancha and Pullammanappallil, 2012), clarity of low frequency Rayleigh wave energy was enhanced by utilizing shorter spacing of 50 m, compared with 100 m or 200 m in the previous study. In total 60 instruments were deployed along each array. The ReMi technique allowed 1D velocity profiles as a function of depth to be obtained along each array. Subsets of 15 instruments were used to obtain a series of 1D velocity-depth sounding from ambient noise recordings. To map depth and characterize lateral velocity heterogeneity beneath each array, these 1D velocity-depth profiles were interpolated to obtain 2D structural representations of shear-wave velocities.

Our efforts in this project allow characterization of the velocity structure beneath a region of the Reno-area basin which has the potential to produce strong ground shaking due to the sediments thickness. Efforts will contribute towards development of the Western Basin and Range Community Velocity model and the Reno-Carson City urban hazard map. As a result, ground-motion modeling capabilities will be improved contributing toward the goal of predicting earthquake ground motions in urban areas and other sensitive sites.

Determination of 3D-velocitystructure across the northeastern portion of the Reno-Area Basin

Aasha Pancha
Optim SDS, 200 South Virginia Street, Suite 560, Reno, NV, 89501
Telephone (775) 236-5869 Fax:(775) 324-5662
Now: at Victoria University of Wellington, Aasha.Pancha@vuw.ac.nz
Satish Pullammanappallil
Optim SDS, 200 South Virginia Street, Suite 560, Reno, NV, 89501
Telephone.: (775) 236-5891 Fax:(775) 324-5662 satish@optimsoftware.com

1. Introduction

1.1 Objectives:

A key component of local seismic hazard assessment is the estimation or quantification of local site response. Existing hazard estimates for Reno area given by the U.S. Geological Survey National Hazard Maps are nominally appropriate for rock sites. This study contributes towards quantifying adjustments to account for local site and basin effects. Current velocity data for the Reno-area basin are limited in resolution to intervals of 1 km to 3 km. As a result, 3D basin details are currently insufficient for ground motion simulation (Pancha *et al*., 2004). Such capabilities are essential for seismic hazard evaluation. This project obtains shallow shear-velocity sections across the northeastern region of the Reno-area basin, where little is known about basin depths and velocity structure. Attempts to compute scenario shaking models for earthquakes affecting Reno, point to a crying need for better definition of the geometry of the Reno-area basin and of the velocities within it. Louie's group at UNR has been building the Nevada ShakeZoning community seismic modeling environment to take advantage of the growing data sets within the Western Basin and Range Community Velocity Model. Three-dimensional, full-wave synthetic ground motions produced by Nevada ShakeZoning have now been validated for Las Vegas against recordings of the 1992 M5.7 Little Skull Mounain earthquake by Flinchum *et al.* (2012). Figure 1 shows that we have had much less success with trial scenario computations in Reno. Despite trying three different basin models, from Abbott and Louie (2000) as shown in Figure 1, through Saltus and Jachens (1995), to Widmer (2005) and Cashman *et al.* (2012), we have failed to match just the peak ground velocities (PGV) recorded at most stations in and around the basin. Figure 1 (right) illustrates that the data-to-model PGV match is not within even a factor of four.

Two seismic arrays, each 2.95 km long, were deployed orthogonal to each other, consisting of 60 wireless instruments placed 50 m apart. The locations of these two lines are shown in Figure 2(a) and 2(b). Application of the Refraction Microtremor (ReMi) technique (Louie, 2001) to ambient noise recorded by the arrays resulted in 1D shallow shear-wave velocity profiles to depths of 600 m to 1000 m with 50 m vertical resolution. A series of 1D velocity soundings along each array allowed 2D velocity representations of the shear-wave velocity structure to be created, mapping the near-surface lateral velocity heterogeneity beneath the arrays. This study builds upon 3D velocity modeling of the deepest western portion of the Reno basin using the ReMi technique under USGS-NEHRP grant award G12AP20026 (Pancha and Pullammanappallil, 2012). The locations of the three arrays obtained under award G12AP20026 relative to the two arrays deployed in this study are shown in Figure 2(a).

The noisy urban setting, logistics, and high cost mean conventional reflection and refraction studies are impractical for imaging to great depths. Use of wireless stand-alone instruments, together with ambient noise, permits long array data to be inexpensively acquired, allowing velocity characterization of these deep sediments. Our efforts contribute towards improving ground motion modeling capabilities and an accurate understanding of earthquake ground motions and their variability in the Reno area.

1.2 Prior efforts to characterize velocity and basin structure in the Reno area

The cities of Reno and Sparks, Nevada, are located in a fault controlled basin that is about 13-km wide and 21-km long. The formal name for the area is the Central Truckee Meadows, referring to the geomorphic flat region of Quaternary deposits. The basin area delineated by gravity, which is shown in Figure 3, is referred to by Abbott and Louie (2000) as the Reno Area basin. The study region considered in this proposal encompasses both these areas, and we refer to it as the Reno Area basin after the largest city in the Reno–Sparks urban area, following Abbott and Louie (2000). The small basin size and the growing ANSS accelerograph network within it make this area a very attractive location for improving modeling techniques to explain the relationship between basin structure, near-surface geology, and ground motions.

The Reno-area basin is a fault-bounded graben, with range front fault zones along the western Sierra Nevada margin and an inferred fault bounding the Virginia Range along the eastern side. Numerous smaller scale faults also exist within the Reno basin, including a "horst and graben" fault structure as discussed by Widmer (2005). The northeastern portion of the basin, which is the focus of this proposal, is estimated to be 600 m deep, based on the initial gravity data set modeled by Abbott and Louie (2000) (Figure 2). More recent gravity modeling of the region utilizes additional data and geological constraints (Cashman *et al*., 2012), indicated that the sub-basin may be shallower. Borehole data are limited, none of which are located over the study region. While both the Abbott and Louie (2000) and Cashman *et al.* (2012) models indicate the existence of a deep sub-basin in the northwest, both models differ in the absolute depth of the basin depth of this region. The difference in the basin depths from gravity results from the various definitions and densities of the bedrock basement unit utilized for each geophysical model.

Abbott and Louie (2000) define the volcanic material of the Kate Peak formation as bedrock with a density of 2.67 g/cc in modeling the basin depth. This is in contrast to Jachens and Moring (1990), who treated the Tertiary Kate Peak volcanics as basin fill, with basement

being the Sierran Granodiorite and older rocks. Cashman *et al.* (2012) made direct measurement of 169 rock densities to define average densities for the nine geological units, and distinguish between the Tertiary volcanics of the Kate Peak formation at 2.5 g/cc, as well as the Cretaceous granite and Mesozoic metavolcanics at 2.7 g/cc and 2.8 g/cc respectively. One major question confronting the assessment of earthquake hazard within the entire Reno-area basin is whether or not the thick (~2 km) Kate Peak deposits act like basin sediments, with the Cretaceous granite beneath acting as the true bedrock from a seismic response point of view. Our deep velocity characterization combined with scenario earthquake modeling can address this issue.

Characterization of velocity within the Reno-Area basin has been limited until present. Prior to 2000, only one seismic sensor was located within the basin. Installation of the current ANSS network (Figure 2) began in 1999 and was completed in 2003. Using over 10,000 events and seismic stations across the northern Nevada/California region, Preston and von Seggern (2007) obtain a 3-D P- and S-wave tomograhpic inversion for the greater Reno-Carson urban corridor with resolution from 3 km to 10 km depth. Cross-correlation of ambient noise for inter-station distances of 0.5 to 60 km (Tibuleac *et al.*, 2009, 2011) allowed for velocities to be determined across the basin but is only resolved on a horizontal grid with 6 km spacing and an initial surface layer thickness of 1 km (Tibuleac, personal communication, 2009).

Efforts to characterize shallow shear-wave velocities throughout the Reno-area basin using the refraction microtremor (ReMi) technique (Louie, 2001) have been ongoing. A transect conducted along the Truckee River (Figure 2) measured 54 shallow shear-wave velocity profiles spaced 300 m apart (Scott *et al.*, 2005), immediately south of the current study region. The aim of the study was to obtain average shallow shear-wave values to 30 m depth (Vs30). Although data to 200 m depth are presented by Scott *et al.* (2005) along the transect length, data beyond 100 m depth is less constrained due to the array length. Additional measurements are archived at www.seismo.unr.edu/vs/archive. These include 21 measurements made by Clark *et al.* (2005) to investigate the potential of a local fault as a hydrological barrier. More recently, ANSS stations within the Reno-Carson urban corridor have been characterized (Pancha *et al.,* 2007), including under USGS-NEHRP sponsorship (external grant award numbers G09AP0051 (Louie) and G11AP20022 (Optim SDS)).

Two seismic profiles were acquired towards understanding the basin structure and fault locations in the area (Frary *et al.*, 2011) as well as S-wave velocity information through analysis of ambient noise using the ReMi technique (Odum *et al.*, 2011). These seismic lines do not traverse the northeastern sub-basin of the Reno area basin, which is the focus of this study.

2. Array Configuration and Data Acquisition:

The objective of the array deployment was to obtain shear-wave velocity information down to 1000 m depth with a depth resolution of 50 m across the northwestern sub-basin (Figure 3). Two orthogonal arrays, 2.95 km long, were installed, as shown in Figure 2. The selected line locations best capture the maximum basin depth and the extent of the sub-basin structure. Each array consisted of 60 wireless instruments, spaced 50 m apart. These standalone Sigma™ cableless acquisition systems manufactured by iSeis (Heath, 2011), shown in Figure 4, were paired to standard vertical geophones with natural frequency of 4.5 Hz. Each seismometer unit location was surveyed using a TopCon GRS-1 mobile handheld unit. Once deployed, and powered on, the Sigma™ units started recording passive data. Each Sigma™ unit has its own

built in memory, so data is stored on each Sigma™ unit independently. As only 60 instruments were available, the two arrays could not be deployed simultaneously. Instead, each line was installed individually on three consecutive days during August, 2014. Each array was deployed for a total time length of three hours, at a sampling rate of 2 milliseconds, during which ambient noise was recorded. After completion of recording each day, the data was downloaded from each unit and concatenated into records for each individual line.

Use of wireless stand-alone instruments together with ambient noise enabled several long array data to be inexpensively acquired, with limited manpower. However, the urban environment necessitated the need for constant security monitoring of the instruments throughout the deployment, placing constraints on the maximum time span of recording due to budget restrictions.

3. Dispersion curve analysis and Shear-Wave Velocity Modeling:

The Refraction Microtremor (ReMi) (SeisOpt® ReMi™, ©Optim 2001-2012) method was used to obtain a series of 1D velocity profiles as function a of depth from the noise records captured by the two orthogonal array lines shown in Figure 2. Refraction microtremor is a volume-averaging surface-wave measurement, averaging velocities where geology is laterally variable, thus differing from single point data obtained from downhole logs. In this method, microtremor noise from sources such as traffic and freeways excites Rayleigh waves, are recorded by a linear array of vertical refraction geophones. The noise records are transformed into slowness–frequency (p-f) space, and a dispersion curve is picked along a minimum-velocity envelope where the gradient of the power spectral ratio is greatest (Louie, 2001; Pancha *et al*., 2008). Modeling of the dispersion curve produces a depth–velocity sounding (Figure 5, top), which can be vertically averaged to the single Vs30 value used by the NEHRP-UBC code. To characterize and map the lateral velocity heterogeneity beneath the area, a series of 1D velocity-depth soundings are and then interpolated to obtain a 2D structural representation of shear-wave velocities such as that illustrated in Figure 5 (bottom). In essence, the 2D image is comprised from a moving array of instruments.

For the current array data, subsets of 15 consecutive geophone instruments used to produce a series of 1D shear-wave velocity depth profiles characterizing average the shallow structure beneath each array line. These "sub-arrays" were spaced along each array, nominally moving two instruments along each line. Where significant changes in the 1D velocity profiles were noted, additional sub-arrays were analyzed to adequate characterize structural changes along the length of each line. Table 1(a) and 1(b) lists the instrument subsets used to obtain 1D velocity soundings along Line 1 and Line 2 respectively. The microtremor data for each sub-array was wavefield-transformed to slowness-frequency space. Rayleigh-wave dispersion of the surface-wave was identified in slowness-frequency space, and a fundamental mode dispersion curve was picked. The dispersion curve was then forward modeled producing a shear-velocity-*vs*.-depth profile for each sub-array.

Ability of the seismic array to image velocity structure at depth depends on the capability of the array to capture ground motion at wavelengths that sample the target depths. The frequency content of the recorded data is dependent on several factors. These include the array length, geophone spacing, sampling rate, geophone frequency, the time length of the data records, and the frequency content of the excited noise sources producing the recorded ground

motions. Typically, the depth of penetration of the recorded wave field is half the array length. To successfully image the velocity profile of the entire sediment package and define the basin depth, time length of the recorded ambient noise required to successfully image Rayleigh-wave dispersion at low frequencies representative of the velocity structure at depth. Based on the results from the study undertaken through under USGS-NEHRP grant award G12AP20026, we decreased the station spacing to 50 m intervals, and used two minute records for the data analysis. Through visual inspection of the ambient noise records, the most favorable record sections with high energy waves were selected for analysis. The combination of closer station spacing and record lengths of two minutes, the resultant dispersion curves are much clearer. The introduction clarity of the dispersion images are illustrated in Figure 6 and Figure 7, where dispersive energy is clearly observed frequencies between 0.5 Hz to 10 Hz.

The reference velocity structure employed for the analysis of data under award G12AP20026 reference models was used to model the shear-velocity structure beneath northwestern Reno-Sparks. The maximum velocity of the bedrock basement of the G12AP20026 study was constrained to values consistent with the deeper velocity structure obtained by Preston and von Seggern (2007) through 3-D P- and S-wave tomograhpic inversion. Use of the G12AP20026 reference velocity-depth profile helped restrict bedrock depths and allow determination of the shallower velocity structure. Depths to the higher velocity bedrock interface are resolved by the dispersion picks.

Velocity models for adjacent sub-arrays along each line were adjusted so that while layer velocities remained relatively unchanged, interface depths were modified. Small adjustments of the layer velocities and the of additional layer interface help match the dispersion curve data where needed. The restriction of layer velocities enhanced the ability to map lateral changes in the velocity structure along each line, and to interpolate these changes across the study area to the perpendicular array. Care was taken to ensure that the models obtained along Lines 1 and 2 were in agreement at the intersection of the two arrays.

The preferred profile will always be the profile interpretation that results in the minimum number of layers to accommodate the observed Rayleigh-wave dispersion and produces a best estimate, reliable and repeatable velocity structure. Because forward modeling is used rather that an inverse method to obtain our velocity-depth models, we are able to test the necessity and sensitivity of the data to both layer thickness and layer velocity. The resultant model is therefore the simplest to explain the data. This follows from Occam's razor principle that "entities must not be multiplied beyond necessity", that simply states, "one should not increase, beyond what is necessary, the number of entities required to explain anything". Over-parameterization of the profile with too many layers complicated the detection of lateral changes in the structure along each array, defeating the purpose of characterizing notable geological features beneath the array.

4. Results

Analysis of the ambient noise recorded by the two arrays beneath the northwestern sub-basin achieved the goal of characterizing shear-wave velocities in the upper 1 km of the surface and determining the basin structure. The 2D shear-wave representations presented in Figures 12 and 13 provide a better depiction of the basement topography and major velocity variations than previously available.

Along Line 1 (Figure 12), basin depth is shown to be much deeper at the southern end of the line with bedrock at approximately 600 m depth. Line 2 intersects Line 1 at approximately 1480 m distance, where basin depth decreases to ~500m. North of this intersection the basin begins to rapidly shallow. At a distance of 1650 m, corresponding the model defined by stations 19 to 48, bedrock shallows from 300 m depth to 200 m depth.

Basin depth at the western end of Line 2 (Figure 13) is uniform at approximately 500m depth until a distance of about 1360 m, where it intersects with Line 1. East of this point, the bedrock depth slowly shallows to 250 m depth at the eastern limit.

5. Contribution towards Seismic Hazard Assessment and Ground motion prediction

Results of this study provide a more thorough characterization of basin structure. The basin depth and shear-wave velocity models presented above help identify areas susceptible to shaking during large earthquake events due to near-surface shear-wave velocity and basin depth. This effort contributes towards development of the Western Basin and Range Community Velocity model and the Reno-Carson City urban hazard map. The final step will be the incorporation of the shear-wave velocity structure into the Nevada ShakeZoning community seismic modeling environment at the Nevada Seismological Laboratory at the University of Nevada, Reno. This will aid improvement in ground-motion modeling capabilities contributing toward the goal of predicting earthquake ground motions in this highly populated and earthquake prone urban region.

Towards assisting development and implementation of the next generation attenuation (NGA) models, using the 1D velocity sounding along each site, values of average velocities Vs10, Vs30, Vs50 and Vs100 to depths of 10, 30, 50, and 100 meters are computed by arithmetic slowness averaging with the formula below:

$$VsZ = \frac{Z}{\sum_{1}^{N} \frac{z_i}{V_i}}$$

where Z is the total depth, z_i is the thickness of layer i with shear velocity V_i. Similarly, we have picked Z0.5, Z1.0, Z1.5, and Z2.0, which are the depths where the shear velocity first exceeds 0.5 km/s, 1.0 km/s, 1.5 km/s, and 2.0 km/s respectively. These values are listed in Table 1(a)-(b). Caution however must be used when using the Vs10 and Vs30 reported in Table 1(a)-(b). The large station spacing means that velocities above 50 m depth are not well resolved. To obtain reliable velocity estimates using ReMi in this depth range, additional arrays with closer station spacing are required. The shorter array lengths allow denser measurements to characterize the near-surface, which likely exhibits greater velocity variations.

6. Conclusions:

Analysis of the ambient noise record recorded by the three arrays presented in Figure 2 successfully achieved the goal of refinement the basin structure and characterization of shear-wave velocities in the upper 1 km of the surface. The 2D shear-wave representations presented in Figures 12and 13 provide a more accurate depiction of the basin shape than previously available. Future studies within the Reno-area basin will benefit from this knowledge, allowing subsequent

arrays to be ideally places to improve our knowledge of the basin structure and the velocities within it. The 2D models do not highlight the location of major structural faults. If present, faults traversed by these arrays do not significantly displace sediments with considerable velocity contrast beneath 50 m depth. While small scale near-surface faults may be present in the upper 50 m, which may manifest appreciable velocity contrasts, due to the station spacing of 50 m, these are not able to be characterized by this study. Array lengths with denser measurements are required to characterize the near-surface.

7. Further Refinements:

One possible caveat of these shear-wave velocity models is the trade-off between velocity and depth. We propose to refine the 2D velocity models through use of cross-correlation and auto-correlation of the ambient noise records to image the geological structure beneath the arrays. Using seismic interferometry through cross-correlation and auto-correlation the P reflection time section from the ambient noise records is recovered. Stacking of these results over time windows will allow generation of a virtual shot gather. Processing of these virtual shot gathers will result in an image of the Earth's reflection response beneath each of the three arrays. Seismic interferometry has been tested through a pilot study with comparison of active source data across two seismic lines gathered in Nevada. Ambient noise data were recorded over three consecutive days at sensors co-located along the location of two active seismic reflection array lines. Comparison of processed noise cross-correlation data with the traditional active seismic reflection record sections show encouraging similarities (Tibuleac *et al.,* 2010). One downfall of that pilot study was the lack of surface ambient noise and poor azimuthal coverage of noise sources. The urban setting of the data analyzed under this proposal overcomes these data limitations, enhancing the potential of obtaining detailed seismic reflection images.

Noise sources from the urban setting of the data from this study will provide detailed waveform data to image subsurface structure. The abundant cultural noise from all azimuths, make this data ideal and affords us a unique opportunity to apply this new imaging method. Depths to prominent material interfaces with high impedance contrasts can be identified from these sections, including the basin bottom. These depths will place additional constraints on the forward modeling of the Rayleigh-wave dispersion data used to invert for the velocity-depth structure beneath each array. The resultant seismic interferometric reflection images may also highlight the existence and location of localized faulting in the area along with other geological features such as discontinuities.

References:

Abbott, R. E., and J. N Louie. (2000). Depth to bedrock using gravimetry in the Reno and Carson City, Nevada area basins, *Geophysics*, 65, 340-350.

Cashman, P. H.,J. H. Trexler, Jr., M. C. . Widmer, and S. J. Queen (21012). Post–2.6 Ma tectonic and topographic evolutionof the northeastern Sierra Nevada: The record in the Reno and Verdi basins *Geosphere*, v. 8, p. 972-990, doi:10.1130/GES00764.1.

Clark, M., J. Louie, A. Pancha, J. Scott, and K. Heath (2005). Geophysical investigation of a fault as a hydrologic barrier in Reno, Nevada: presented at the Seismol. Soc. of Amer. Ann. Mtg., Lake Tahoe, Nevada, April 26-29.

Flinchum, B. A., W. H. Savran, K. D. Smith, J. N. Louie, S. K. Pullammanappallil, and A. Pancha, (2012). Validation of Las Vegas basin response to the 1992 Little Skull Mtn. earthquake as predicted by physics-based Nevada ShakeZoning computations, presented at *Seismological Society of America Annual Meeting*, San Diego, April 17. On line at: http://crack.seismo.unr.edu/ma/validation/Flinchum-SSA12.html

Frary, R. N., J. N. Louie, W. J. Stephenson, J. K. Odum, L. Liberty, S. Pullammanappallil, N. Prina, P. Cashman, J. Trexler, and R. L. Kent (2001). 3D Controls on Basin Structure from a Network of High-Resolution Seismic Imaging Profiles in South Reno, Nevada, *Abstract, Sesismological Research Letters*, 82(2), 298, presented at the *Seismological Society Annual Meeting*, 13-15 April, Memphis, Tennessee.

Heath, R. (2011). Time to consider the practicalities of passive seismic acquisition, *First Break*, 29 (7), 91-98.

Louie, J. N. (2001). Faster, better: Shear-wave velocity to 100 meters depth from refraction microtremor arrays, *Bull. Seism. Soc. Amer., 91*, 347-364.

Louie, J.N., M. Thompson, S. Hauksson, Z. Reynolds, E. Hall-Patton, E., and S. Pullammanappallil, (2009). Shear-velocity measurements at CISN stations along the southern San Andreas Fault, Final Technical Report to the U.S. Geological Survey, National Earthquake Hazards Reduction Program, award no. G09AP00050, variously paginated.

Odum, J. K., W. J. Stephenson, R. N. Frary, G. C. Schmauder, and J. N. Louie (2001). Shallow 3.5 km Long, Shear-wave Velocity Profile in Reno, Nevada Derived from Ambient Noise Analysis of Uncorrelated P-wave Minivib Data, *Abstract, Sesismological Research Letters*, 82(2), 299, presented at the *Seismological Society Annual Meeting*, 13-15 April, Memphis, Tennessee.

Pancha, A., J.G. Anderson, J.N. Louie, and A. Anooshehpoor (2004). Data and simulation of ground motion for Reno, Nevada, 13th World Conference on Earthquake Engineering, Vancouver, B.C., Canada, Aug. 1-6, 2004, Paper No. 3452.

Pancha, A., J. Anderson, and J. Louie (2007). Characterization of near-surface geology at strong-motion stations in the vicinity of Reno, Nevada, *Bull. Seismol. Soc. Amer., 97*, 2096-2117, doi: 10.1785/0120060266.

Pancha, A., J. G. Anderson, J. N. Louie, S. Pullammanappallil, (2008).Measurement of shallow shear wave velocities at a rock site using the ReMi technique, *Soil Dynamics and Earthquake Engineering*, 28, 522-535.

Pancha, A., and S. Pullammanappallil (2012). Determination of 3D-velocitystructure across the deepest portion of the Reno-Area Basin, *Final Report to the National Earthquake Hazard Reduction Program*, U. S. Geological Survey Award Number G12AP20026, 2012.

Preston, L., and D. von Seggern (2008), Joint Seismic Tomography/Location Inversion in the Reno/Carson City Area, *Final Report to the National Earthquake Hazard Reduction Program*, U. S. Geological Survey Award Number 07HQGR0022.

Saltus, R. W., and R. C. Jachens (1995). Gravity and basin-depth maps of the Basin and Range Province, Western United States, U.S. Geological Survey, *Geophysical Investigations Map, Report: GP-1012,* 1 sheet.

Scott, J. B., M. Clark, T. Rennie, A. Pancha, H. Park, and J. N. Louie (2004). A shallow shear-wave velocity transect across the Reno, Nevada area basin, *Bull. Seismol. Soc. Amer.*, 94, 2222-2228.

Stephenson, W. J., R. N. Frary, J. N. Louie, and J. K. Odum (2012). Extensional growth faulting beneath Reno, Nevada, imaged by urban seismic profiling, [in review].

Tibuleac, I. M., D von Seggern, J Louie and J Anderson (2009). High resolution seismic velocity structure in the Reno basin from ambient noise recorded by a variety of instruments, *Geothermal Resources Council 3rd Annual Meeting*, Oct 4-7, 2009, Reno NV, U.S.A.

Tibuleac, I.M.; Pullammanappallil, S.; von Seggern, D. H.; Pancha, A.; Louie, J. N., (2010). Retrieval of Earth's reflection response from ambient seismic noise - a Nevada experiment, *American Geophysical Union, Fall Meeting 2010*, Abstract #S33A-2071

Tibuleac, I. M., D. H. von Seggern, John G. Anderson and J.N. Louie, 2011. Computing Green's Functions from Ambient Noise Recorded by Narrow-Band Seismometers, Accelerometers, and Analog Seismometers, *Seism. Res. Lett.*, 82, 661-675. doi: 10.1785/gssrl.82.5.661
http://crack.seismo.unr.edu/ileana/GF_ambient_noise_paper_final.pdf

Widmer, M. (2005). Gravity-based geological modeling of the Central Truckee Meadows, prepared for The Central Truckee Meadows Remediation District, Washoe County Department of Water Resources.

Widmer, M. C., Cashman, P. H., Benedict, F. C., and J. H. Trexler (2007). Neogene through Quaternary Stratigraphy and Structure in a Portion of the Truckee Meadows Basin: A Record of Recent Tectonic History, presented at the *Geological Society of America Cordilleran Section*, 103rd Annual Meeting.

Table 1(a): Instrument groupings used to obtain 1D shear-wave velocity soundings along Line 1 (see Figure 2 for location). Average velocities to 10-, 30-, 50-, and 100-meter depths, denoted $Vs10^{\S}$, $Vs30^{\S}$, $Vs50$, and $Vs100$, respectively are listed along with the depths where the shear velocity first exceeds0.5 km/s, 1.0 km/s, 1.5 km/s, and 2.0 km/s (Z0.5, Z1.0, Z1.5, and Z2.0 respectively).

Station Spread	Midpoint		Velocity, m/s				Depth, m			
	Latitude	Longitude	$Vs10^{\S}$	$Vs30^{\S}$	$Vs50$	$Vs100$	Z0.5	Z1.0	Z1.5	Z2.0
1 to 30	-119.7151	39.5349	329	329	366	419.88	140	492	492	492
3 to 32	-119.7151	39.5359	329	329	366	419.88	140	492	492	492
4 to 33	-119.7150	39.5364	309	309	348	407.84	120	535	535	535
5 to 34	-119.7150	39.5368	323	323	360	415.96	135	595	595	595
6 to 35	-119.7151	39.5373	323	323	358	415.03	137	610	610	610
7 to 36	-119.7151	39.5377	323	323	346	406.89	135	682	682	682
8 to 37	-119.7151	39.5382	316	316	327	393.49	137	627	627	627
9 to 38	-119.7151	39.5386	343	343	343	404.46	135	627	627	627
10 to 39	-119.7151	39.5391	336	336	336	399.68	135	595	595	595
11 to 40	-119.7151	39.5395	336	336	336	399.68	135	510	510	510
13 to 42	-119.7152	39.5404	329	329	335	398.79	135	492	492	492
15 to 44	-119.7151	39.5413	329	329	335	398.79	135	492	492	492
17 to 46	-119.7151	39.5424	295	295	336	399.32	115	412	412	412
19 to 48	-119.7151	39.5432	316	316	327	393.49	117	297	297	297
21 to 50	-119.7149	39.5441	316	316	327	395.86	97	292	292	292
23 to 52	-119.7149	39.5450	316	316	327	393.49	100	287	287	287
25 to 54	-119.7149	39.5459	316	316	327	393.49	100	270	270	270
27 to 56	-119.7149	39.5468	316	316	316	384.87	102	240	240	240
29 to 58	-119.7149	39.5477	309	309	309	384.20	95	221	221	221
31 to 60	-119.7151	39.5486	309	309	309	379.76	105	212	212	212

[§] Due to the large station spacing, velocities above 50 m depth are not well resolved.

Table 1(b): Instrument groupings used to obtain 1D shear-wave velocity soundings along Line 2 (see Figure 2 for location). Average velocities to 10-, 30-, 50-, and 100-meter depths, denoted $Vs10^\S$, $Vs30^\S$, $Vs50$, and $Vs100$, respectively are listed along with the depths where the shear velocity first exceeds0.5 km/s, 1.0 km/s, 1.5 km/s, and 2.0 km/s (Z0.5, Z1.0, Z1.5, and Z2.0 respectively).

Station Spread	Midpoint		Velocity, m/s				Depth, m			
	Latitude	Longitude	$Vs10^\S$	$Vs30^\S$	Vs50	Vs100	Z0.5	Z1.0	Z1.5	Z2.0
1 to 30	-119.7219	39.5418	253	268	297	363	270	492	492	492
2 to 31	-119.7213	39.5418	253	268	297	358	250	492	492	492
4 to 33	-119.7201	39.5419	244	272	300	364	247	492	492	492
6 to 35	-119.7188	39.5419	261	268	297	363	247	492	492	492
8 to 37	-119.7177	39.5418	261	268	297	363	247	492	492	492
10 to 39	-119.7164	39.5418	261	268	297	363	247	492	492	492
12 to 41	-119.7152	39.5418	261	268	297	363	216	492	492	492
14 to 43	-119.7140	39.5418	261	265	295	366	172	432	432	432
16 to 45	-119.7129	39.5418	261	265	295	366	177	385	385	385
18 to 47	-119.7116	39.5418	261	265	295	366	177	385	385	385
20 to 49	-119.7104	39.5418	248	263	294	365	170	315	315	315
22 to 51	-119.7093	39.5418	248	263	294	367	175	307	307	307
24 to 53	-119.7081	39.5418	248	263	294	368	175	307	307	307
26 to 55	-119.7068	39.5417	248	263	294	368	142	257	257	257
28 to 57	-119.7057	39.5418	248	267	297	370	157	257	257	257
30 to 59	-119.7045	39.5418	248	267	297	370	147	235	235	235
31 to 60	-119.7038	39.5418	254	266	284	379	136	203	203	203

[§] Due to the large station spacing, velocities above 50 m depth are not well resolved.
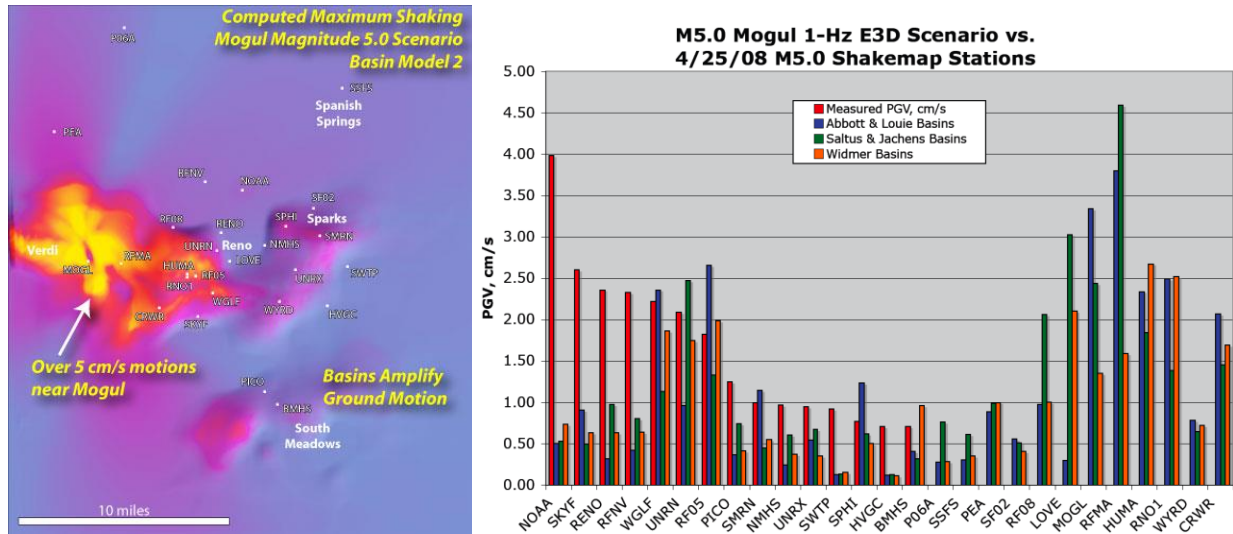
Figure 1: Results of a trial 3D scenario model of the M5 4/25/08 Mogul main shock, computed to a maximum frequency of 1.0 Hz. (left) Peak ground velocity (PGV) map resulting from the Nevada ShakeZoning community seismic modeling environment, with Abbott and Louie (2000) basin structure in shaded relief. (right) PGV recorded at named stations (red bars), not matched by Nevada ShakeZoning 3D predictions using 3 different basin models.
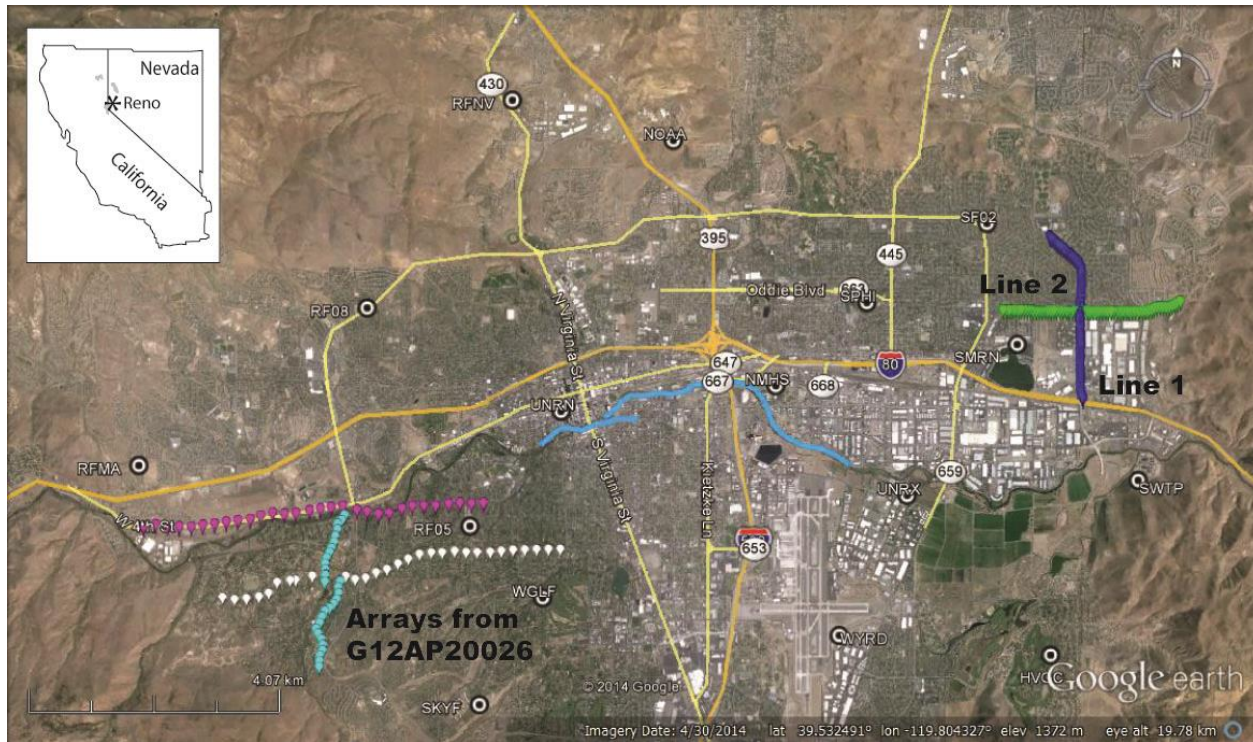
Figure 2(a): Locations of two deep refraction microtermor (ReMi) arrays are shown in purple (Line 1) and green (Line 2). These new lines complement data acquired across the deepest portions of the basin (see Figure 2) under grants G12AP20026 (magenta, light blue, and white). Sixty wireless instruments were deployed at 50 m spacing along the 2.95 km long arrays to record ambient noise. Reflection lines acquired by Stephenson *et al.* (2013) and Frary (2012) along the Truckee River are shown in cyan. ANSS station locations (white dots) are also shown. The two northwestern arrays for this study, Line 1 and Line 2, are shown in detail in Figure 2(b). Inset shows the geographic location of Reno, Nevada, U.S.A.

Figure 2(a): Locations of two deep refraction microtermor (ReMi) arrays are shown shown in purple (Line 1) and green (Line 2). Sixty wireless instruments were deployed at 50 m spacing along the 2.95 km long arrays to record ambient noise. Numbers indicate the station numbering along each array
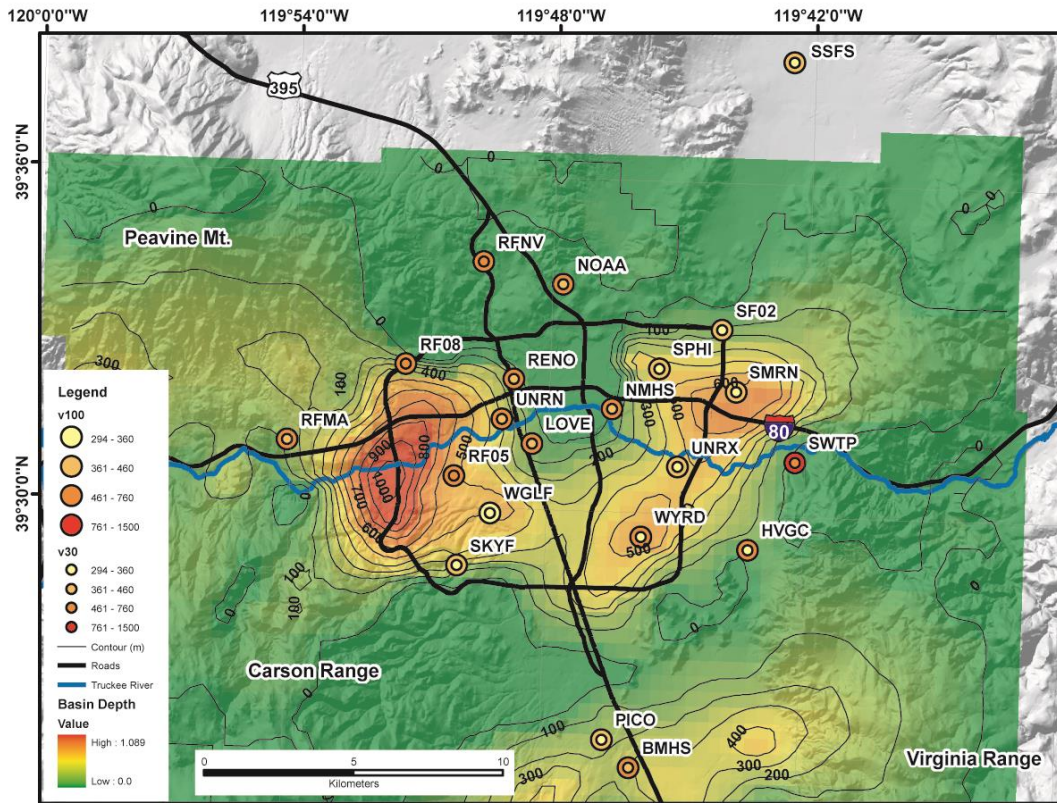
Figure 3: Basin depth model from Abbott and Louie (2000), based on gravity observations. Contours are 100 m. The formal name for the area is the Central Truckee Meadows, referring to the geomorphic flat region of Quaternary deposits. We refer to it as the Reno area basin after the largest city in the Reno–Sparks urban area, following Abbott and Louie (2000), incorporating both the geophysical and geomorphic expression of the basin.

Figure 4: Pictures showing the Sigma™ cableless acquisition system by iSeis (Heath,2011). Each is powered by a 12-V battery and is connected to a single vertical P-wave geophone for this study.
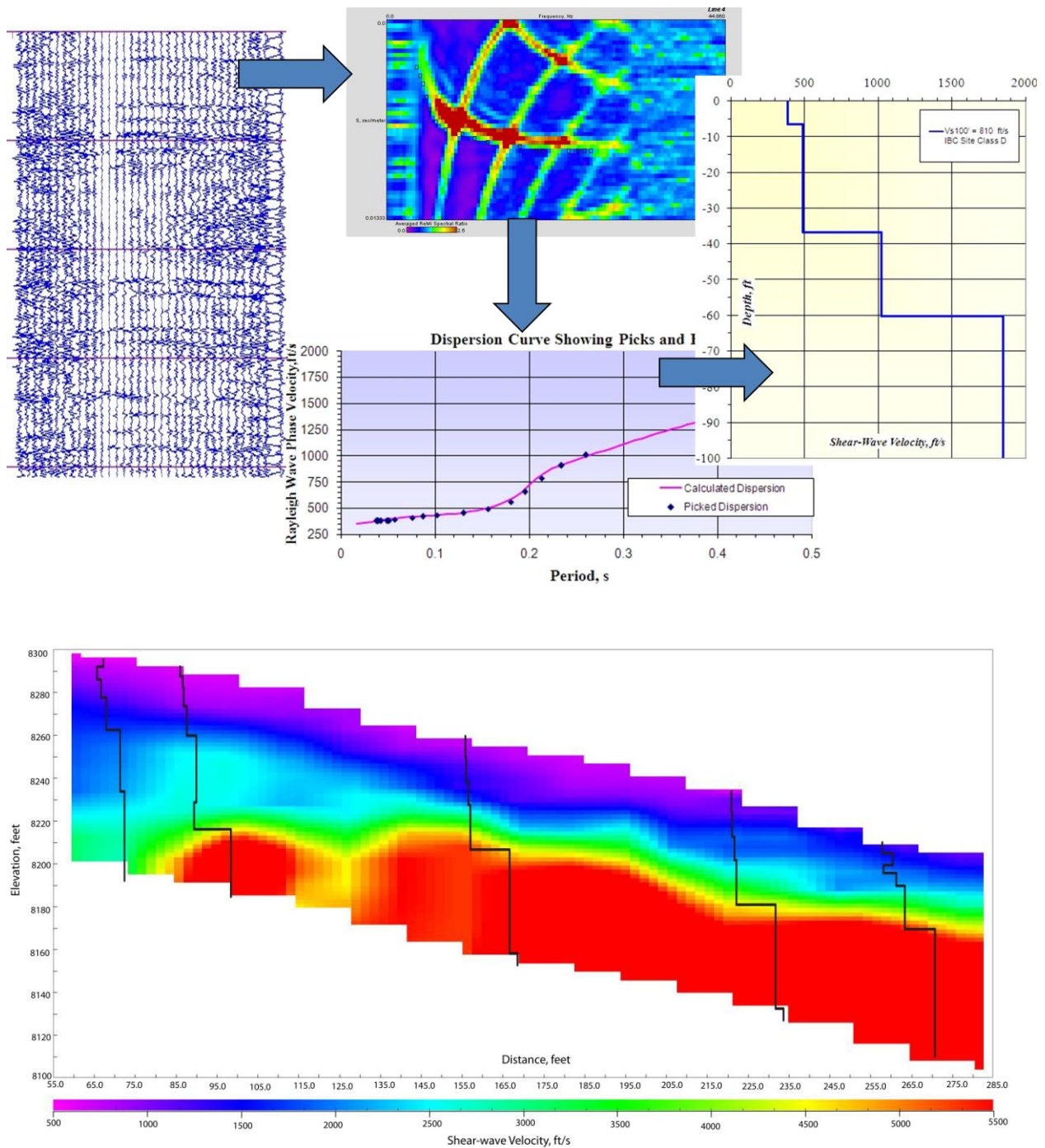
Figure 5. (top) Schematic of the ReMi™ process. Recorded microtremor data are first transformed into the frequency-slowness domain (Louie, 2001). The dispersion curve is then picked and modeled to obtain a 1D shear-wave velocity profile.

(bottom) Example of 2D Vs velocity modeled determined using 2D refraction microtremor analysis. The solid lines are the 1D profiles which are then interpolated to derive the 2D velocity structure. This image was produced using Optim's SeisOpt® ReMi™ software. The same technique will be employed to produce similar images along the locations proposed in Figure 3.
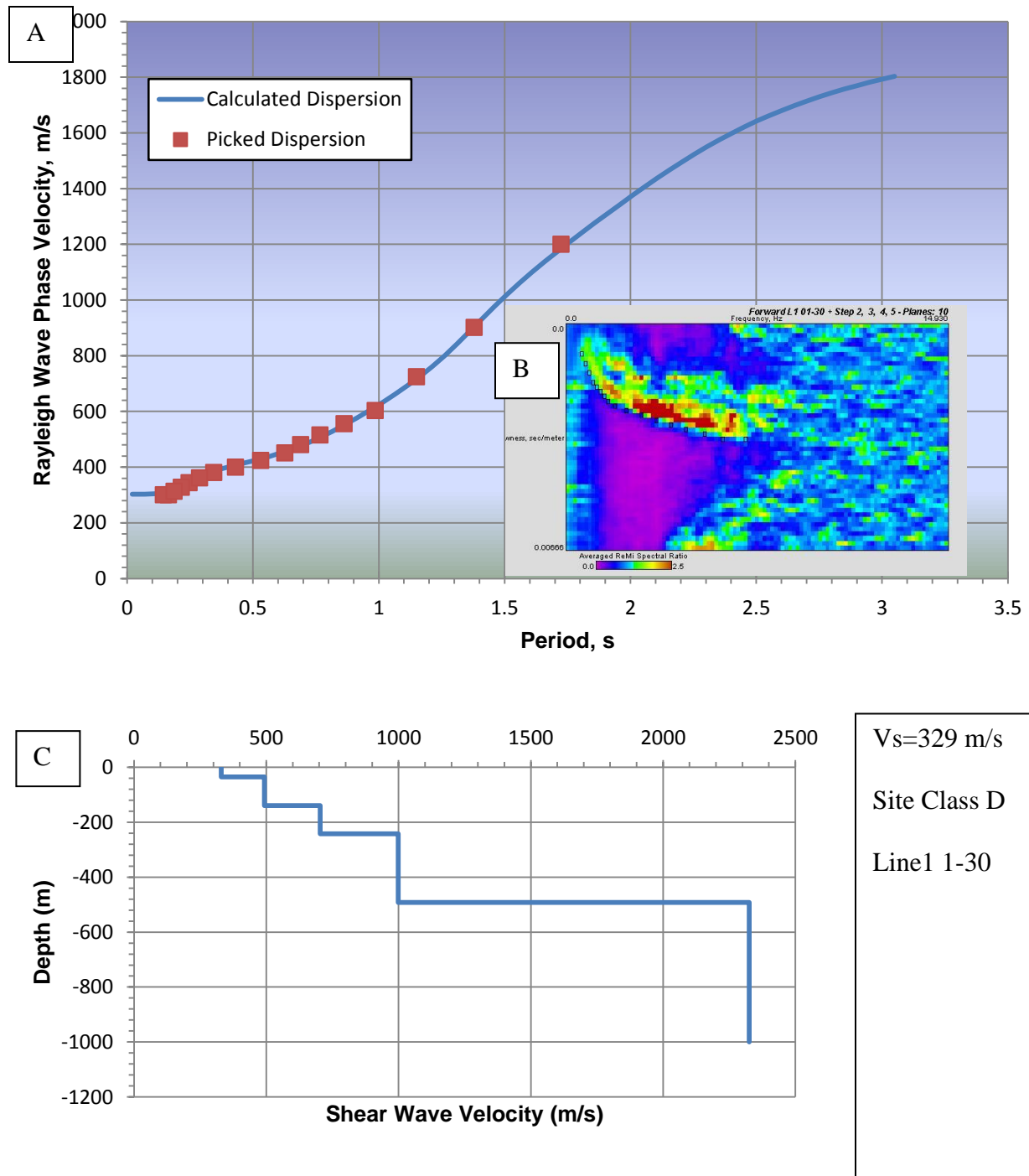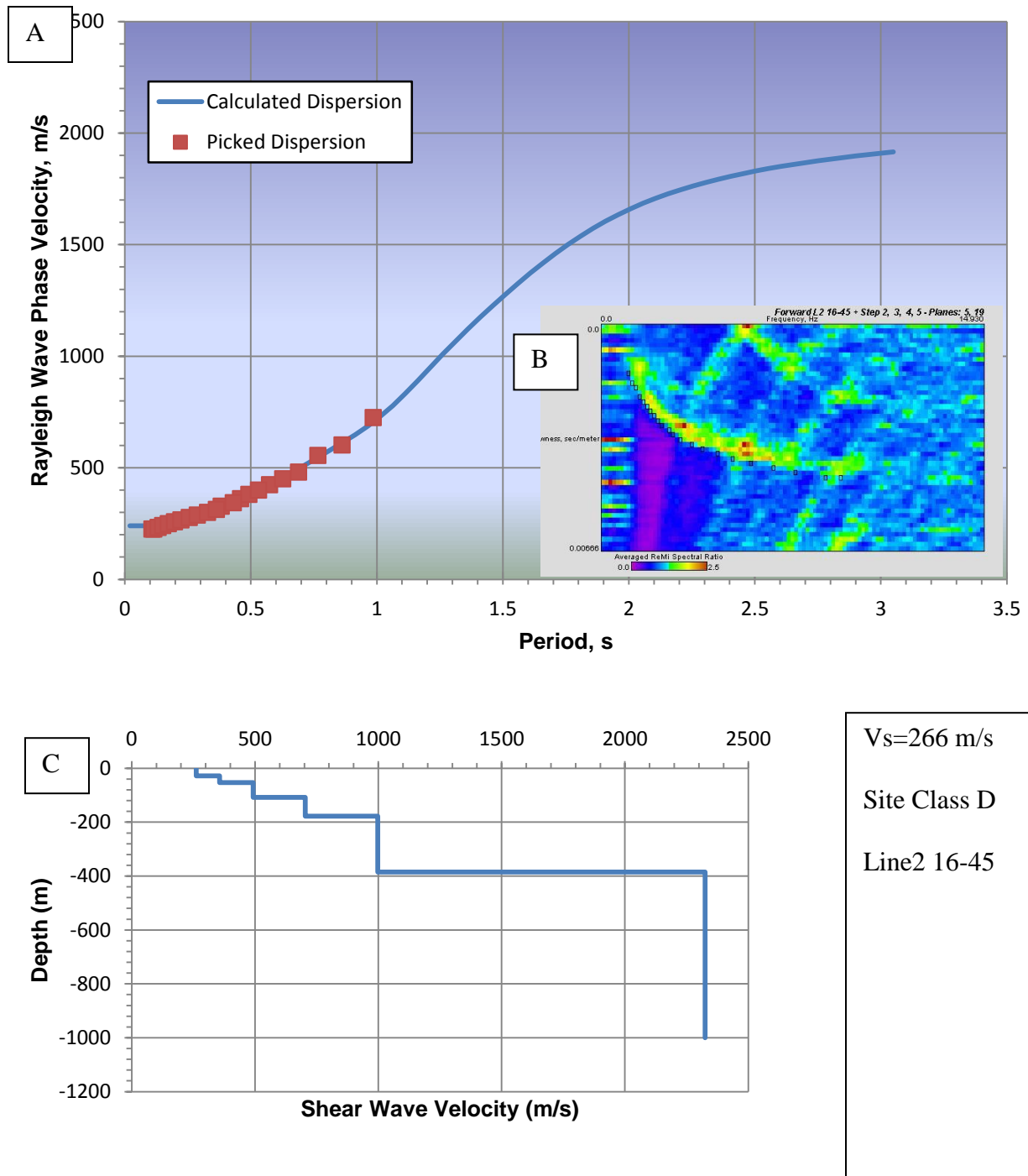
Figure 6: Example of ReMi analysis for a sample record along Line 1 1-30. Recorded microtremor data are first transformed into the frequency-slowness domain (Louie, 2001) (**A**). The dispersion curve is then picked (**B**) and modeled to obtain a 1D shear-wave velocity profile (**C**).
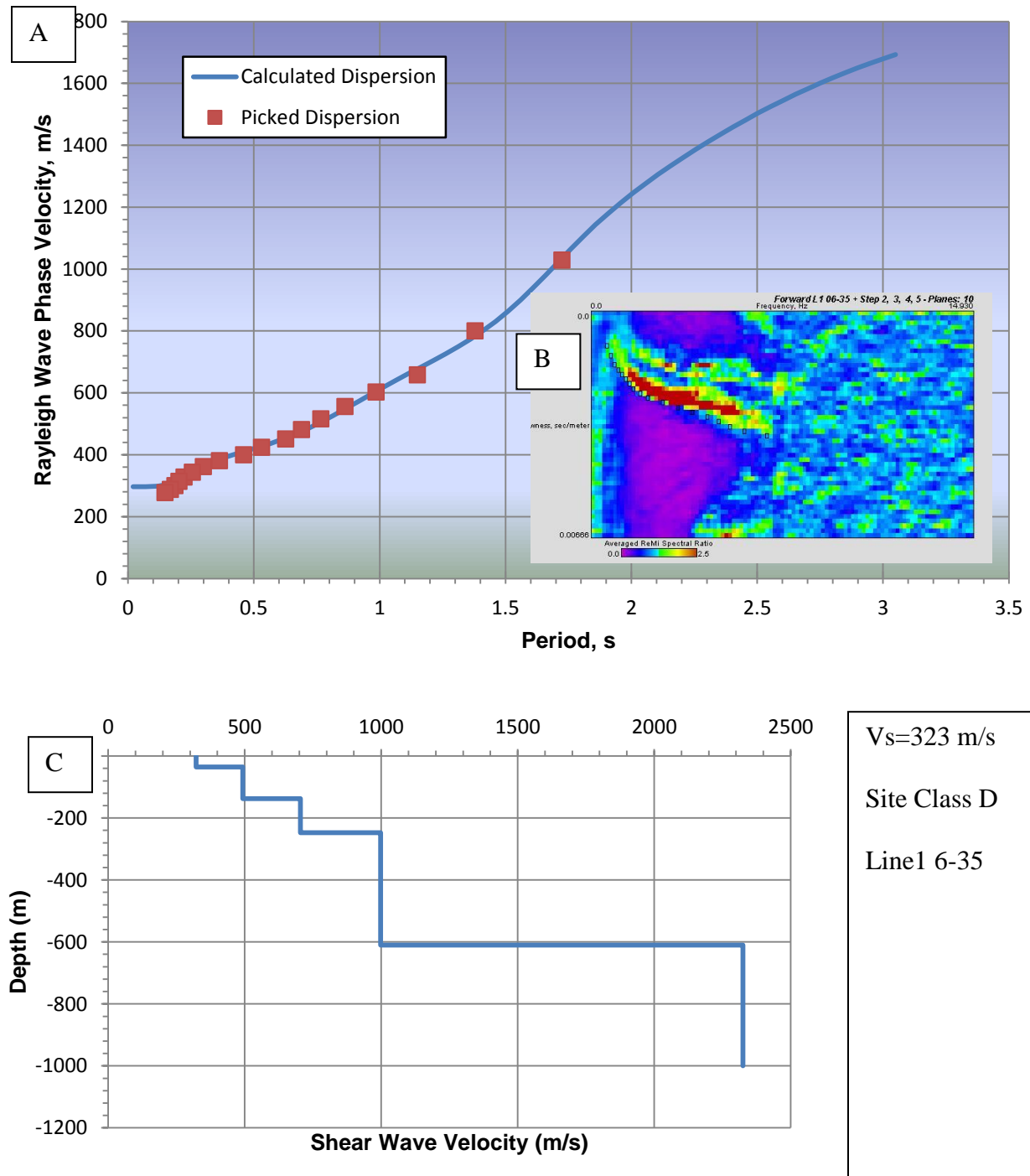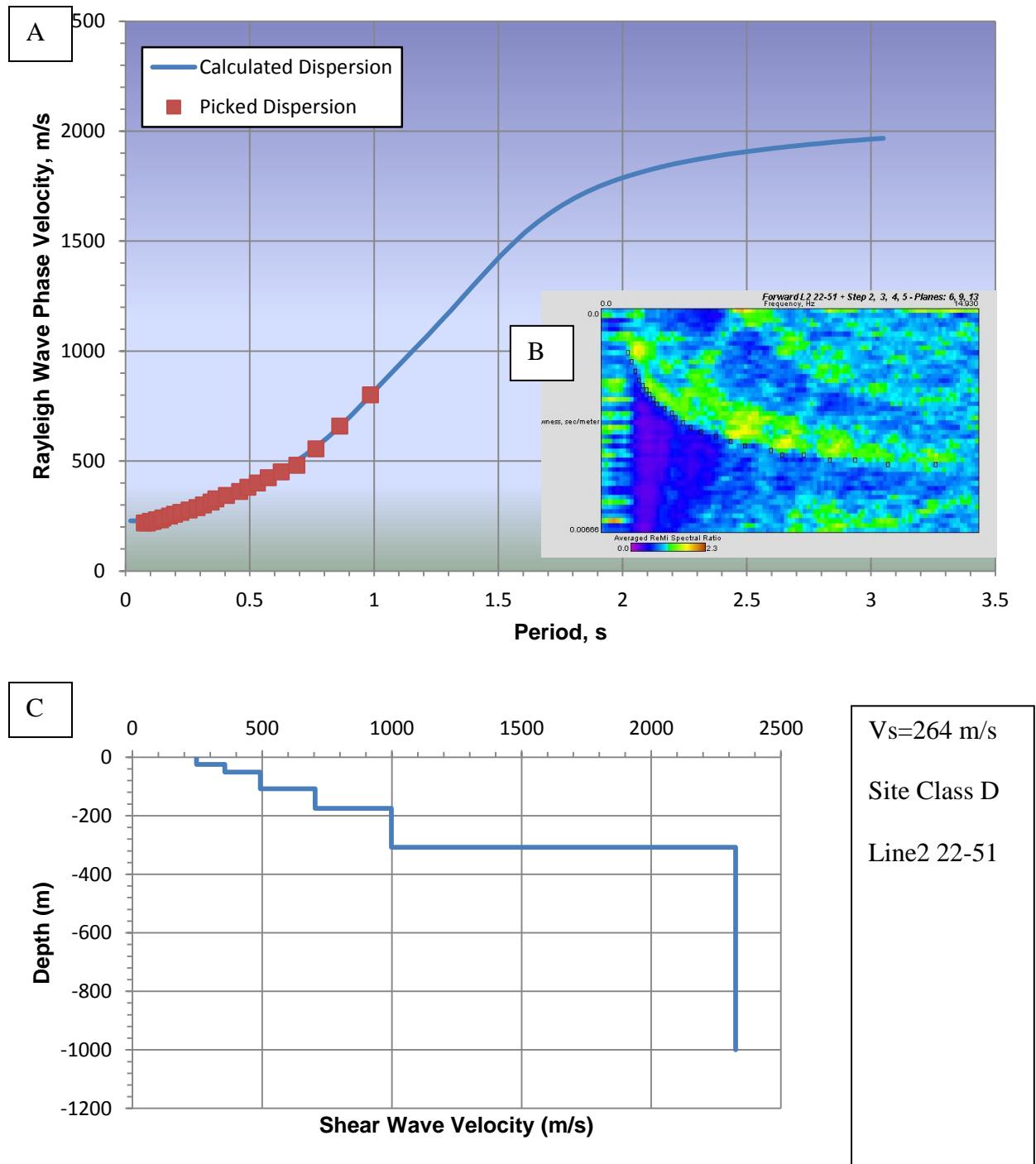
Figure 7: Example of ReMi analysis for a sample record along Line 1. Recorded microtremor data are first transformed into the frequency-slowness domain (Louie, 2001) (**A**). The dispersion curve is then picked (**B**) and modeled to obtain a 1D shear-wave velocity profile (**C**).
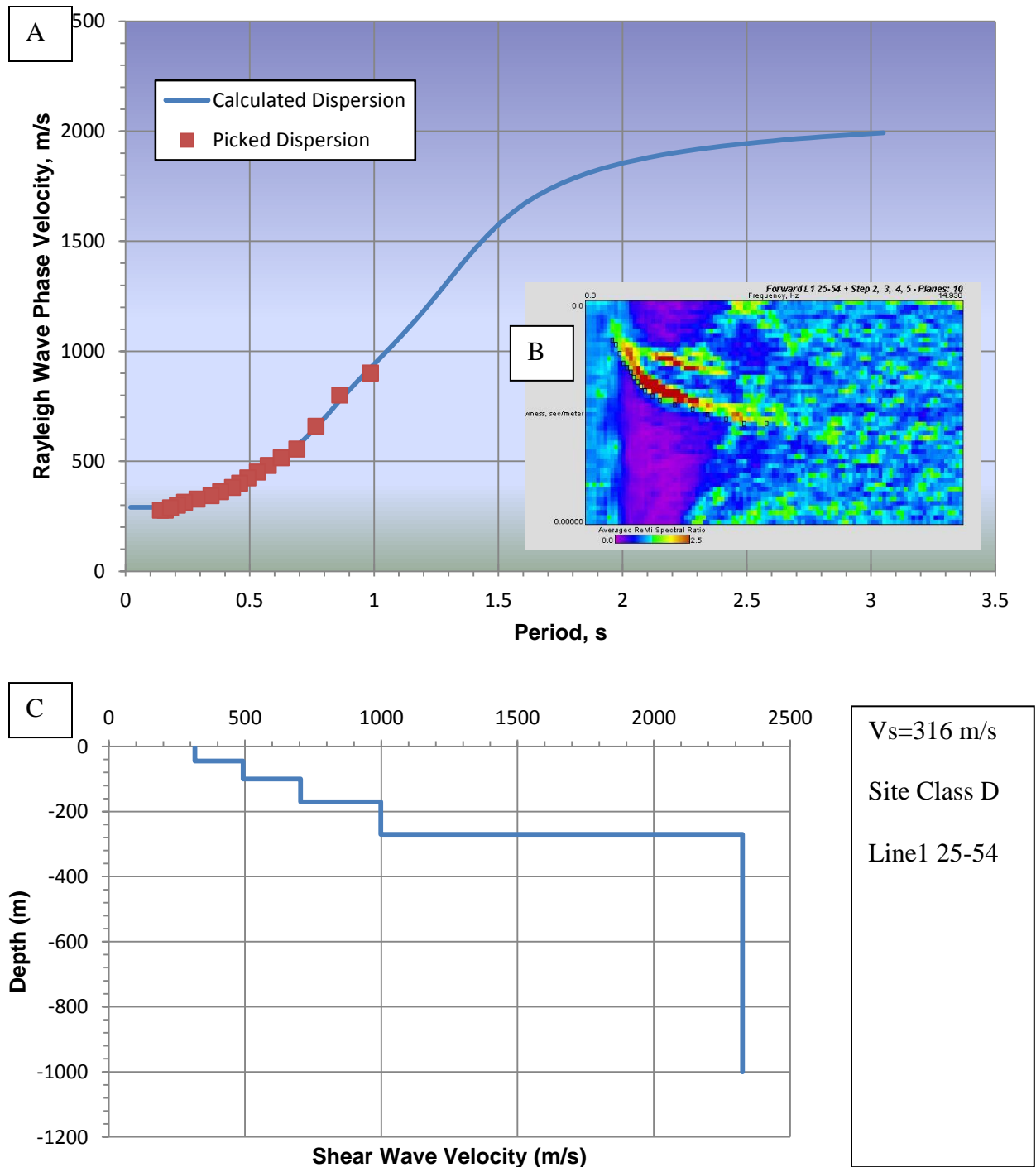
Figure 8: Example of ReMi analysis for a sample record along Line 1. Recorded microtremor data are first transformed into the frequency-slowness domain (Louie, 2001) (**A**). The dispersion curve is then picked (**B**) and modeled to obtain a 1D shear-wave velocity profile (**C**).
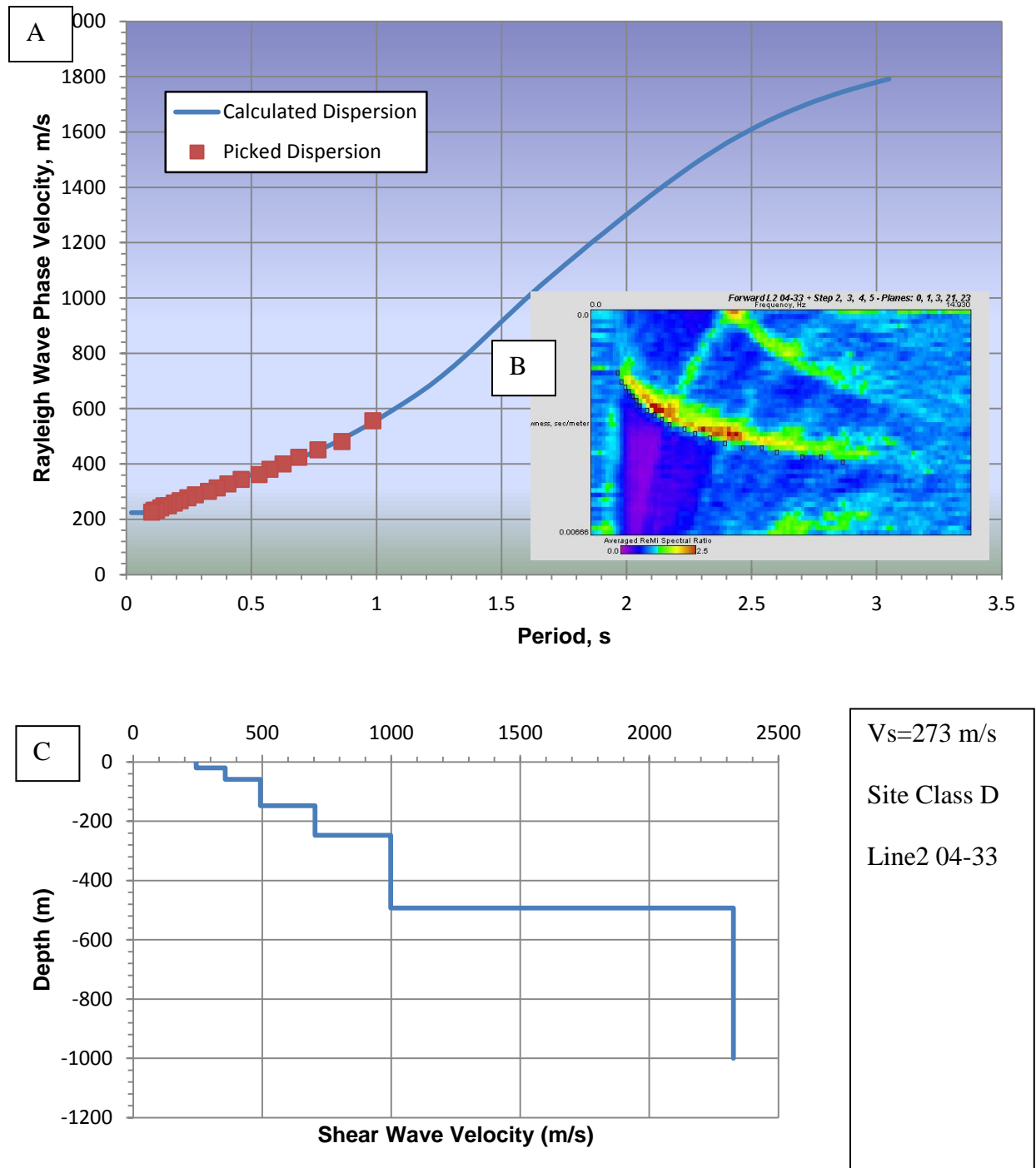
Figure 9: Example of ReMi analysis for a sample record along Line 2 04-33. Recorded microtremor data are first transformed into the frequency-slowness domain (Louie, 2001) **(A)**. The dispersion curve is then picked **(B)** and modeled to obtain a 1D shear-wave velocity profile **(C)**.

Figure 10: Example of ReMi analysis for a sample record along Line 2 16-45. Recorded microtremor data are first transformed into the frequency-slowness domain (Louie, 2001) **(A)**. The dispersion curve is then picked **(B)** and modeled to obtain a 1D shear-wave velocity profile **(C)**.

Figure 11: Example of ReMi analysis for a sample record along Line 2 22-51. Recorded microtremor data are first transformed into the frequency-slowness domain (Louie, 2001) **(A)**. The dispersion curve is then picked **(B)** and modeled to obtain a 1D shear-wave velocity profile **(C)**.
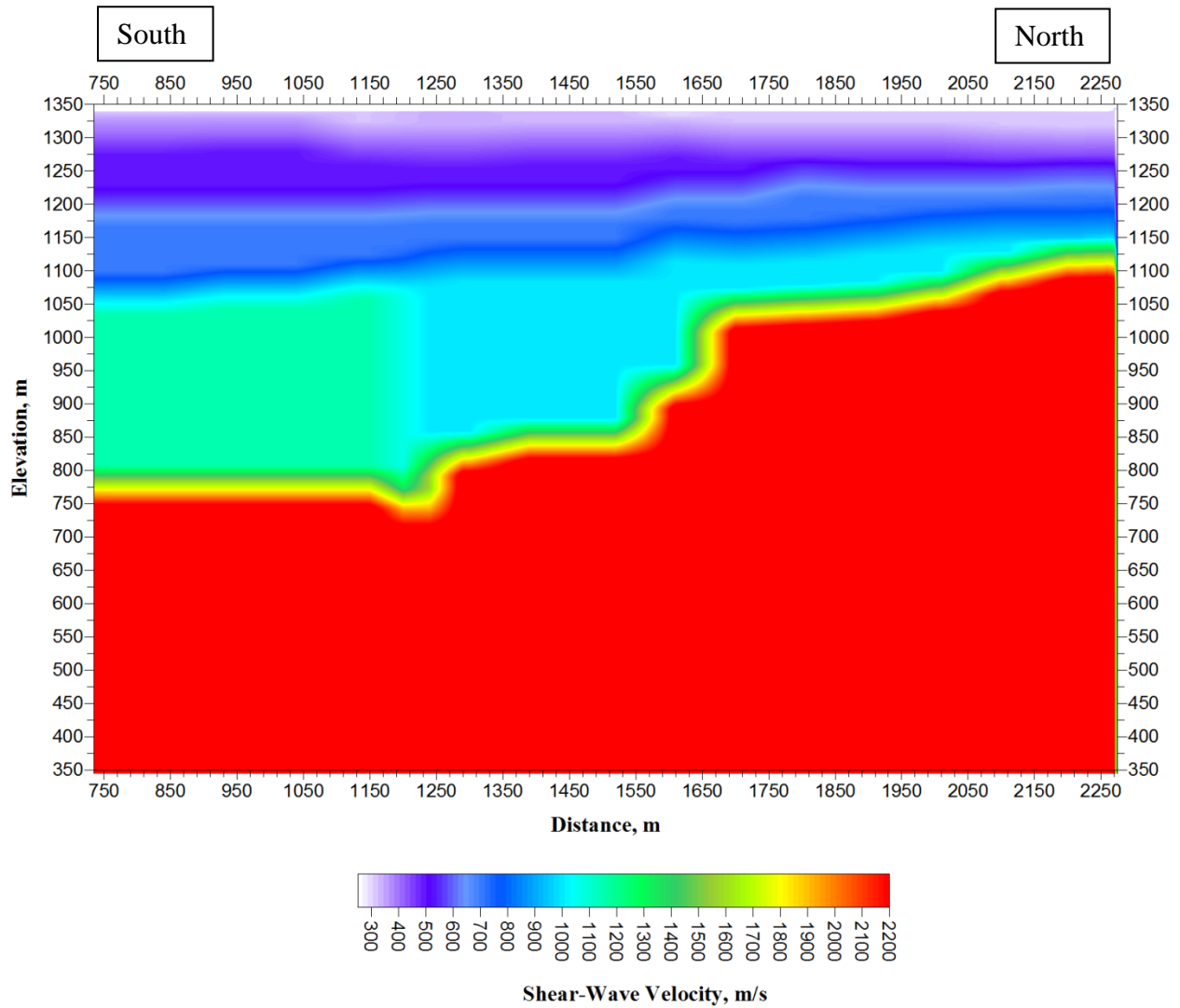
Figure 12: 2D Vs velocity modeled determined using 2D refraction microtremor analysis for Line 1. The image is compiled through interpolation of 1D shear-velocity profiles as function of depth determined from a moving array of 15 instruments along each line length. Distances along the array (assuming Station 1 is located at 0 m) are show along the bottom. The vertical axis shows elevation with top of the model at 1350 m.
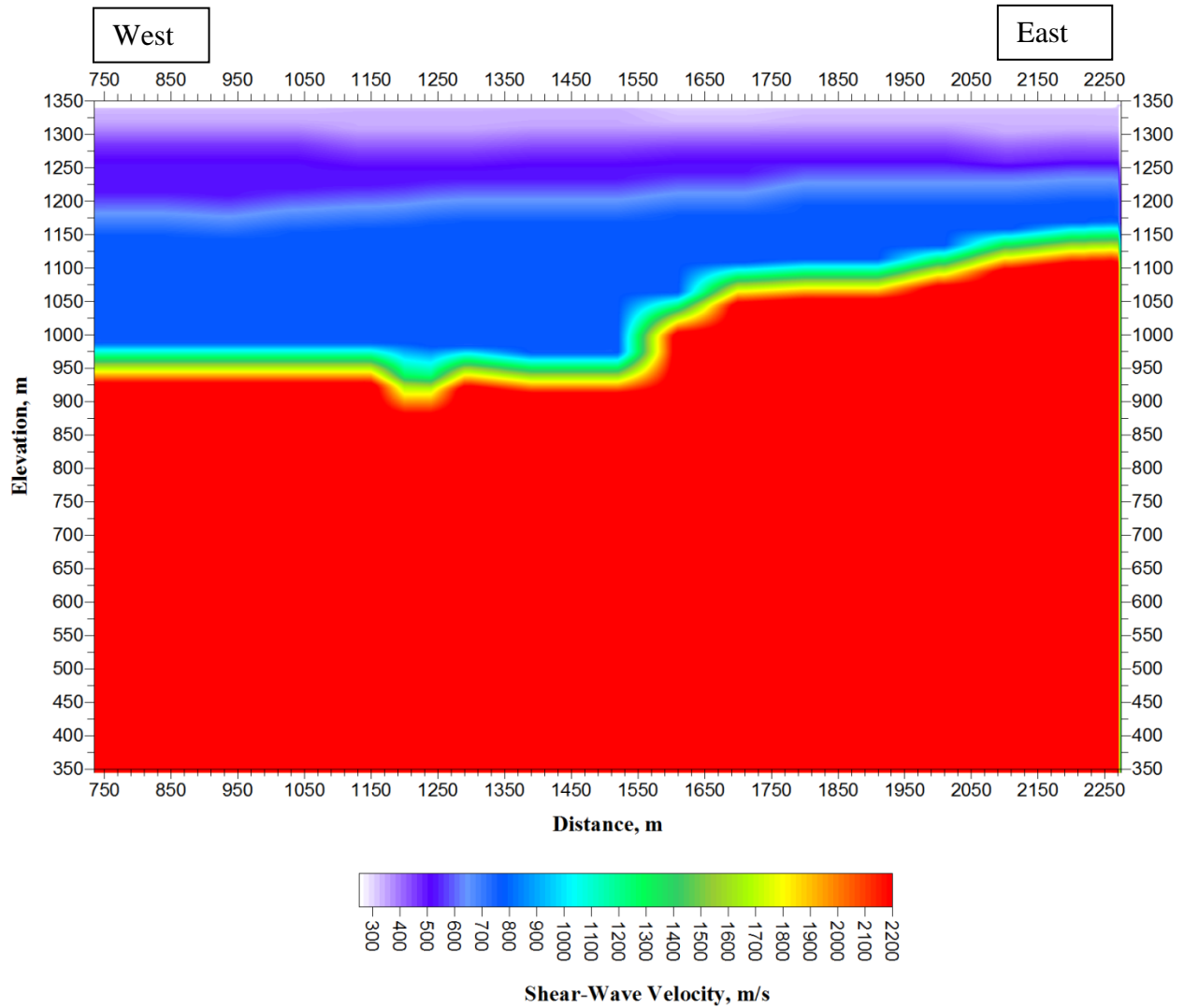
Figure 13: 2D Vs velocity modeled determined using 2D refraction microtremor analysis for Line 2. The image is compiled through interpolation of 1D shear-velocity profiles as function of depth determined from a moving array of 15 instruments along each line length. Distances along the array (assuming Station 1 is located at 0m) are show along the bottom. The vertical axis shows elevation with top of the model at 1350 m.